

Improved Current Densities in MgB₂ By Liquid-Assisted Sintering

S. K. Chen, Z. Lockman, M. Wei, B. A. Glowacki

and J. L. MacManus-Driscoll

Department of Materials Science and Metallurgy, University of Cambridge,

Pembroke Street, Cambridge CB2 3QZ, UK

Polycrystalline MgB₂ samples with GaN additions were prepared by reaction of Mg, B, and GaN powders. The presence of Ga leads to a low melting eutectic phase which allowed liquid phase sintering and produces plate-like grains. For low-level GaN additions ($\leq 5\%$ at. %), the critical transition temperature, T_c , remained unchanged and in 1T magnetic field, the critical current density, J_c was enhanced by a factor of 2 and 10, for temperatures of $\sim 5\text{K}$ and 20K , respectively. The values obtained are approaching those of hot isostatically pressed samples.

MgB₂ is an intermediate temperature, type II superconductor with T_c of $\sim 40\text{K}$, and with promising applications potential in high field magnets, motors and magnetic resonance imaging. It is now well known that high grain boundary angles do not produce weakly linked grain boundaries. Hence, instead of focusing on texture improvement (as for high temperature superconductors), materials engineering approaches have been directed towards either improving J_c by improving grain connectivity, or improving in-field performance by alloying or addition of flux pinning centres.

Several hot pressing studies have been conducted on MgB₂, using either hot uniaxial or hot isostatic pressing (HIP) ¹⁻⁶ and have shown improvements in J_c by a factor of 6 at 5K, 4T ³. For possible future MRI applications of MgB₂ which require fields near 2T to be generated and operation temperatures around 20-26K to be used, the improvements in J_c through alloying are small, and it is the microstructure and sample density which dominate the current carrying capacity.

The aim of this work is to study the effect of the addition of Ga to Mg and B precursor powders on the microstructure and hence current carrying capacity of MgB₂ in low fields, of interest for MRI. Of course any enhancements in current carrying capacity at low fields will also be useful in alloyed samples of interest for higher field applications. Hence, the idea of this work is to replicate the promising results of hot pressing studies by using a simple ambient pressure reaction process. Ga forms a low melting (422°C) eutectic liquid with Mg and hence there is the possibility of achieving liquid phase sintering. We used GaN as reactant in the precursor powder as, unlike pure Ga or other salts of Ga, it is easy to handle and is not hygroscopic. In addition, it is known to decompose below 800 °C in the presence of H₂ gas ⁷, namely below the standard reaction temperature used for phase formation of MgB₂.

Doped MgB₂ pellets were prepared by in-situ reaction of Mg (Alfa Aesar, 99.6%), GaN (Aldrich, 99.99+%) and B (Alfa Aesar, 96-98%) powders. GaN of 0, 1, 3, and 5 mol % were added to the Mg and B powders. After manual grinding, the samples were uniaxially pressed at 10 ton/cm². Pellets (5 mm diameter x 2 mm thickness) were encapsulated in Ta foil (Advent, 99.9%) packed with powder of the same composition as the sample, and magnesium metal turnings. The envelope was then placed on a niobium-lined alumina boat. Reaction sintering was undertaken in a tubular furnace under a flowing 2% H₂-N₂ gas mixture. Samples were reacted at 950°C for 15 minutes using heating and cooling rates of 15°C/min.

X-ray diffractometry was conducted using Cu-K α radiation in the Bragg Brentano configuration to determine phase composition of the samples. Field emission gun scanning electron microscopy (FEG-SEM) was undertaken on fracture cross sections of samples to determine samples microstructures. Electron dispersive x-ray analysis (EDX) was also undertaken in the SEM. High resolution transmission electron microscopy (TEM) was undertaken on thinned pellet samples.

Superconducting transition temperatures were recorded using an AC Susceptometer. J_c of the samples was determined using a D.C. SQUID Magnetometer. The sample (around 1 mm³ in volume) was placed in a small capsule, and inserted into the magnetometer. The magnetometer was cooled to around 5 K using liquid helium. Measurements of magnetisation (M) versus magnetic field (H) were recorded on both whole pelletised, fully reacted samples. J_c was determined using the Bean model and the whole sample dimension for the current length scale. Room temperature resistivity measurements were conducted in the Van der Pauw geometry. Density measurements were carried out by weighing the samples, and normalising by the sample geometric volume.

Figure 1 shows the Mg-Ga phase diagram in the composition and temperature region of interest to this study. A eutectic liquid is formed at 422°C, for 19.1 at.% Ga in Mg. Since we have GaN in our precursor mix, it is necessary first to decompose the GaN to Ga+N₂ before the liquid phase can form. According to phase stability studies of GaN in the presence of H₂, any significant decomposition will not occur below 700°C. Hence, the liquid phase will form in the same reaction temperature regime as the MgB₂ forms from the Mg and B precursors. If we assume that MgB₂ begins to form at as low as 550°C⁹, then at just below this temperature, for a 3 at. % Ga sample Fig. 1 indicates that there is 10 mol. % liquid, 30 mol. % Mg, and 60 mol % B. As the temperature increases, the amount of liquid phase will increase but its percentage will depend on the rate of MgB₂ formation compared to heating rate.

Figure 2 compares x-ray diffraction patterns for 0 %, 1 at. % and 3 at. % GaN added MgB₂ samples. The pure and 1 at. % samples show clean x-ray patterns with peaks ascribed to MgB₂ only. The 3 at. % sample shows peaks from Mg₅Ga₂ (and possibly also Mg₂Ga₅ and MgGa₂) and Mg-B-N phases (e.g. Mg₃BN₃ and Mg₃N₂). Hence, the N₂ evolved from the GaN decomposition is not all transported away by the flowing gas, i.e. at least some of it reacts with Mg and B. From the x-ray patterns, there is no measurable preferential alignment of the MgB₂ grains in any of the samples. The 5 at. % sample (not shown) displays the same peaks as the 3 at. % sample, but there are larger quantities of second phase present.

Figure 3 compares FEGSEM fracture micrographs of a pure MgB₂ sample and of two different regions of a 3 at. % GaN sample (b and c). The grain morphologies of the pure (a) and doped (b) samples are strikingly different, with larger, more platy grains observed for the GaN doped samples. The appearance of a cracked surface-covering phase in c) with grains observed below the phase suggests the presence of a

quenched, non-metallic liquid phase with partial surface oxidation. The regions covered $\sim 20\%$ of the fracture surface. Indeed, EDX indicated the composition of the surface layer to be $\text{MgGa}_{2-2.5}$. Fig. 3 (d) shows a high resolution image of a grain boundary region in a 3 at. % GaN sample. An amorphous region is apparent at the grain boundary. Again, these regions are common throughout the sample, and are much more numerous than in the pure sample. The amorphous phase is likely the same covering phase as seen in (c).

Table 1 shows T_c , room temperature resistivity, density, and grain size values for 0–5 at. % GaN doped samples. While T_c does not change with GaN addition (indicative of no substitution of Ga in the lattice), the resistivity shows a systematic increase from $28 \mu\Omega\cdot\text{cm}$ to $102 \mu\Omega\cdot\text{cm}$. The resistivity of the pure sample is typical for the purities of the starting powders employed¹⁰. The sample density also increases systematically, although the density increase is small compared to what one typically achieves by hot pressing ($\sim 2.1 \text{ g/cm}^3$, which is $\sim 80\%$ of the theoretical value)². The grain size increases from the 0% to 1% doped sample but changes little with further doping.

Figure 4 compares J_c versus applied magnetic field up to 3T (// to the radial direction of the sample) for the whole pellets of the pure sample, the 3 at. % doped sample (the highest J_c sample of all the samples prepared), a typical, clean uniaxially pressed MgB_2 sample from the literature¹¹ and a HIP'ed sample from the literature⁴. Fig. 4 (a) shows our data at 6K compared to others at 4.2K, and 5K. The two uniaxially pressed, pure MgB_2 samples show near identical behaviour. The HIP'ed sample has the highest J_c over the whole field regime. J_c ($\sim 5\text{K}$, 1T) is $1 \times 10^5 \text{ A}\cdot\text{cm}^{-2}$, $2 \times 10^5 \text{ A}\cdot\text{cm}^{-2}$, and $4 \times 10^5 \text{ A}\cdot\text{cm}^{-2}$ for the uniaxial pure sample, 3 at. % GaN sample, and HIP'ed pure sample, respectively. Up to 2T, a field range of interest for MRI, the

3 at. % GaN sample shows approximately a factor of 2 improvement over the pure sample, and is approximately half the value of the HIP'ed sample. At 20K, the 3 at. % GaN sample shows a much stronger improvement in J_c over the pure sample. J_c (20K, 1T) is 3×10^4 A.cm⁻², 3×10^5 A.cm⁻², and 5×10^5 A.cm⁻² for the uniaxial pure sample, 3 at. % GaN sample, and HIP'ed pure sample, respectively. The field dependences of the samples are similar which is expected since none of the samples are alloyed.

For the HIP'ed sample, J_c is improved through significant sample densification and grain connectivity. For the GaN added sample, the density is only marginally increased (by around 8% for the 3 at. % sample). The resistivity and second phase fraction both increase with GaN addition. In addition, TEM shows the presence of amorphous regions. These observations are consistent with obstruction of the current path by the second phases, and hence reduced connectivity. The improved J_c must, therefore, originate from an increased intragrain J_c , i.e. improved carrying properties of the grains themselves. This is consistent with the observation of grains with a highly crystalline, faceted nature which are formed through liquid phase sintering. Hence, even though the current carrying cross section is reduced, the overall J_c is still higher because of the enhanced intragranular properties. Attempts to measure intragrain J_c by forming finely crushed powders were not successful for these samples because the finest powder particles obtained (few micron) were more than an order of magnitude larger than the grain size.

In summary, liquid phase sintering has been used to enhance the current carrying properties of bulk MgB₂. The technological significance of improving current carrying capacity without using expensive and size- limiting hot pressing equipment is clear¹¹.

- ¹ A. Handstein, D. Hinz, G. Fuchs, K.-H. Muller, K. Nenkov, O. Gutfleisch, V. N. Narozhnyi, and L. Schultz, *J. Alloys and Compounds* **329**, 285 (2001).
- ² A. Gumbel, J. Eckert, G. Fuchs, K. Nenkov, K.-H. Muller, and L. Schultz, *Appl. Phys. Lett.* **80**, 2725 (2002).
- ³ A. Serquis, X. Z. Liao, Y. T. Zhu, J. Y. Coulter, J. Y. Huang, J. O. Willis, D. E. Peterson, F. M. Mueller, N. O. Moreno, J. D. Thompson, V. F. Nesterenko, and S. S. Indrakanti, *J. Appl. Phys.* **92**, 351 (2002).
- ⁴ X. L. Wang, S. Soltanian, M. James, M. J. Qin, J. Horvat, Q. W. Yao, H. K. Liu, and S. X. Dou, *Physica C* **408-410**, 63 (2004).
- ⁵ A. Tampieri, G. Celotti, S. Sprio, R. Caciuffo, and D. Rinaldi, *Physica C* **400**, 97 (2004).
- ⁶ N. A. Frederick, S. Li, M. B. Maple, V. F. Nesterenko, and S. S. Indrakanti, *Physica C* **363**, 1 (2001).
- ⁷ D. D. Koleske, A. E. Wickenden, R. L. Henry, J. C. Culbertson, and M. E. Twigg, *J. Crys. Growth* **223**, 466 (2001).
- ⁸ T. Massalski, *Binary alloy phase diagram* (A.S.M. International, Materials Park, OH, 1990)
- ⁹ N. Rogado, M. A. Hayward, K. A. Regan, Y. Wang, N. P. Ong, H. W. Zandbergen, J. M. Rowell, and R. J. Cava, *J. Appl. Phys.* **91**, 274 (2002).
- ¹⁰ X. Song, V. Braccini, and D. C. Larbalestier, *J. Mat. Res.* **19**, 2245 (2004).
- ¹¹ V. Braccini, L. D. Cooley, S. Patnaik, D. C. Larbalestier, P. Manfrinetti, A. Palenzona, and A. S. Siri, *Appl. Phys. Lett.* **81**, 4577 (2002).

Table 1 T_c , room temperature resistivity, density and grain size of pure and doped samples.

GaN doped sample	T_c (K)	Resistivity (290K), ρ ($\mu\Omega$.cm)	Density (g.cm^{-3})	Grain size (μm)
0%	38.9	27.8	1.16	0.13 – 0.44
1%	38.9	56.2	1.22	0.53 – 0.96
3%	38.8	61.1	1.25	0.45 – 0.87
5%	38.8	102.1	1.31	0.35 – 0.65

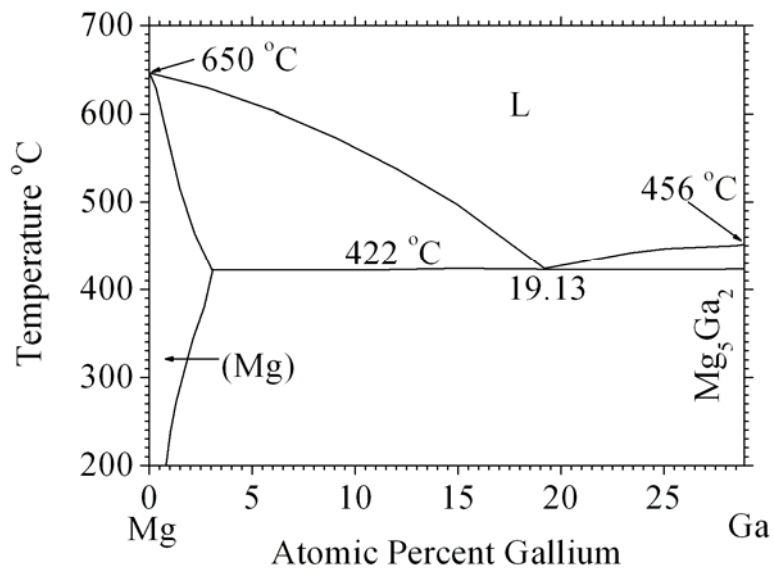


FIG. 1. Mg-Ga phase diagram (after T. Massalski, Ref. 8).

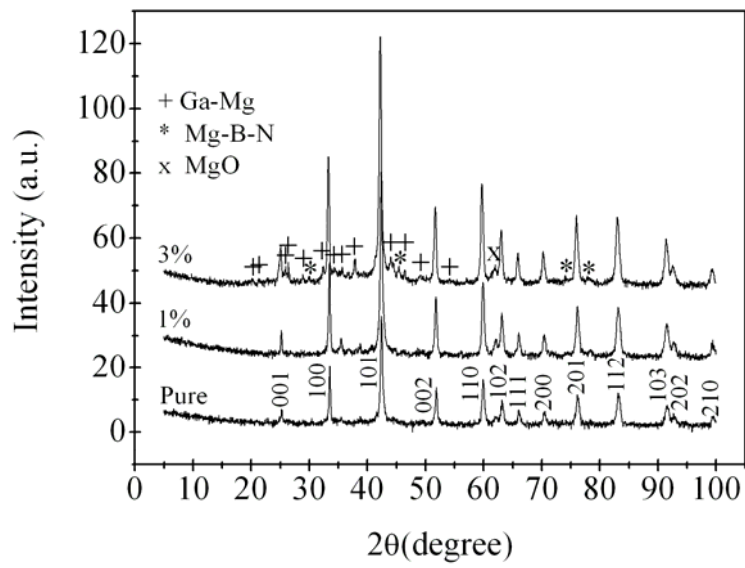


FIG. 2. X-ray diffraction patterns of the pure and GaN doped samples.

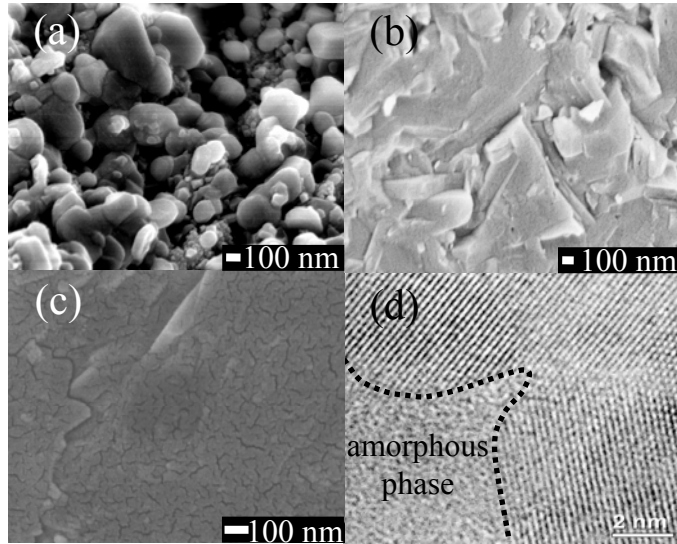


FIG. 3. SEM images of (a) pure MgB_2 , b & c) 3 at.% GaN doped samples at different magnification and (d) TEM image of a grain boundary region in the 3 at. % GaN doped sample.

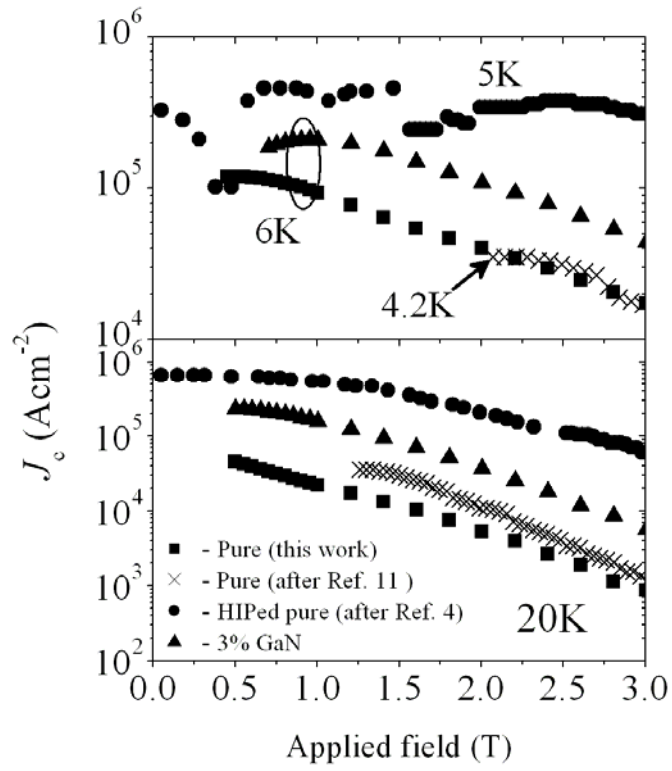


FIG. 4. Comparison of J_c versus applied magnetic field for samples in this work and from literature (Ref. 4); (Ref. 11).